

## Silica encapsulated SERS nanoprobe conjugated to the bacteriophage tailspike protein for targeted detection of *Salmonella*<sup>†</sup>

Li-Lin Tay,<sup>\*a</sup> Ping-Ji Huang,<sup>b</sup> Jamshid Tanha,<sup>a</sup> Shannon Ryan,<sup>a</sup> Xiaohua Wu,<sup>a</sup> John Hulse<sup>a</sup> and Lai-Kwan Chau<sup>\*b</sup>

Received 11th October 2011, Accepted 14th November 2011

DOI: 10.1039/c1cc16325f

**Silica-encapsulated Raman-reporter embedded SERS nanoprobes, named nanoaggregate embedded beads (NAEBs), were conjugated to the *Salmonella* specific tailspike protein (TSP) isolated from the P22 bacteriophage to enable a highly specific and ultrasensitive optical transduction platform. We demonstrate three successful surface conjugation strategies and highlight the detection of a single bacterium using SERS.**

Rapid screening, detection and identification of pathogenic bacteria have a key impact in public health, specifically, in the diagnosis of infectious diseases, food and water safety as well as prevention of bioterrorism. Conventional culture based biochemical and serological assays are highly effective in the identification of microorganisms but suffer from the disadvantages of being time consuming, costly, and labour intensive protocols. Recent advances in the design and fabrication of nanomaterials coupled with target specific surface functional ligands serve as attractive alternatives for the screening and identification of microorganisms.<sup>1</sup> Surface enhanced Raman scattering (SERS) based biosensors and bioassays provide a high sensitivity, rapid and target specific scheme for detection of microorganisms.<sup>2</sup> A SERS based detection scheme has comparable sensitivity to the fluorescence bioassay with the added advantages of photostability and easy multiplex detection. Narrow Raman peaks minimize spectral overlapping and allow a larger number of spectrally distinguishable signatures. Furthermore, excitation of multiple fluorophores with non-overlapping fluorescence bands cannot be easily accomplished by a single wavelength while multiple Raman labels can be excited by just one wavelength.

We have previously demonstrated the fabrication of a SERS active nanoprobe, NAEB, containing Raman reporters adsorbed on a small nanoparticle aggregate and embedded in a protective silica shell.<sup>3</sup> NAEB is a stable colloid fabricated through controlled aggregation of Au nanoparticles (NPs). The slight aggregation is necessary in generating the strong SERS signal which results from the coupling of localized surface plasmon resonances of individual

Au NPs.<sup>4</sup> Fig. 1 shows a typical transmission electron microscopy (TEM) image of NAEB and the corresponding SERS spectrum of the reporter molecule DTDC (3'-diethylthiadicarbocyanine iodine). The inset of Fig. 1B shows the molecular structure of DTDC. Most of the NAEBs range from 100 to 150 nm in size and typically contain between 2 to 6 Au NPs in the core surrounded by a thick silica shell. The silica shell protects the SERS nanoprobe from collapsing in the biological buffers and prevents the displacement of Raman reporters. Our design also allows additional flexibility in the surface conjugation without affecting the SERS optical properties. Herein, we report that NAEB conjugated to a *Salmonella* specific bacteriophage protein functions as a highly specific and sensitive SERS nanoprobe for the targeted detection of *Salmonella*. We present three conjugation schemes for cross-linking the functional moieties of NAEB to the specially engineered bacteriophage protein and demonstrate SERS detection of *Salmonella* down to the limit of a single bacterium.

Specificity of the biosensor depends to a large degree on the selection of appropriate antibodies. Polyclonal antibodies such as IgGs, though popular, exhibit stability and specificity problems.<sup>5</sup> An example of this is shown in Fig. S1 (ESI<sup>†</sup>) where the *Salmonella*-recognizing IgG conjugated to NAEB showed cross-reactivity to both *Salmonella* (target) and *Staphylococcus aureus* (control). In this study, we improved the targeting specificity of the NAEB substantially by conjugating it to the specially engineered tailspike proteins (TSPs) from a P22 bacteriophage that recognizes *Salmonella*.<sup>6</sup> Bacteriophages are typically host specific, self-replicating viruses. P22 TSP is the component of the tail apparatus of P22 bacteriophages that

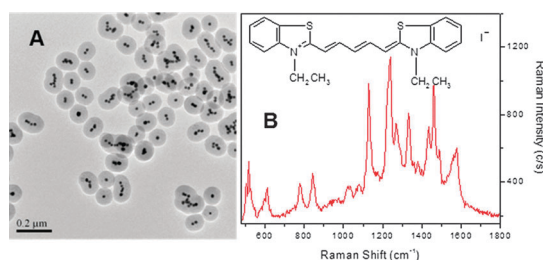


**Fig. 1** TEM image of NAEB (A) and its corresponding SERS spectrum (B). Inset of (B) shows chemical structure of a DTDC Raman reporter molecule.

<sup>a</sup> National Research Council Canada, Ottawa, Canada.

E-mail: [llin.tay@nrc-cnrc.gc.ca](mailto:llin.tay@nrc-cnrc.gc.ca); Tel: +1-613-993-3919

<sup>b</sup> Department of Chemistry and Biochemistry,

National Chung Cheng University, Chia-Yi, Taiwan.

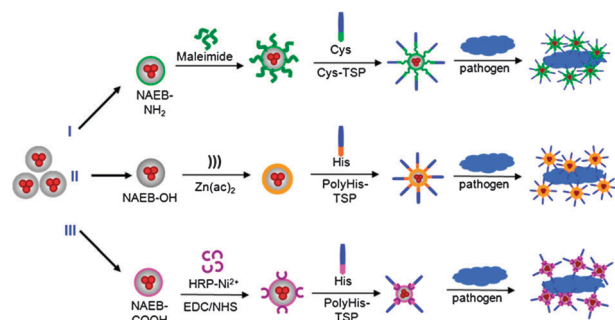
E-mail: [chelkc@ccu.edu.tw](mailto:chelkc@ccu.edu.tw); Tel: +886-5272-0411 X66411

† Electronic supplementary information (ESI) available. See DOI: [10.1039/c1cc16325f](https://doi.org/10.1039/c1cc16325f)

mediates the specific recognition of its host bacteria by binding to the polysaccharides present on the host cell surface. A hallmark of the TSPs is their stability and specificity.<sup>7</sup> TSPs exhibit high thermal stability and are resistant towards proteases and chemical denaturants such as sodium dodecyl sulfate and urea. More specifically, the TSP used in this study is a truncated (180 kDa) and mutated trimeric protein which has the same binding affinity as the full length, wild type version towards the O-antigen of *Salmonella*.<sup>6</sup> Multiple TSPs can be conjugated to the surface of a single NAEB resulting in a multivalent nanoprobe. The multivalency encourages the binding of multiple antigens on a single NAEB thus facilitating both the agglutination assay as well as SERS detection. The TSP used in this study is also genetically engineered to express a cysteine followed by a polyhistidine tag (His<sub>6</sub>) at its N-terminus.<sup>6</sup> We have utilized both moieties to conjugate TSP onto NAEBs.

Scheme 1 outlines the three conjugation strategies that we have successfully demonstrated, showing both the crosslinking of TSP to NAEB as well as the subsequent SERS detection of *Salmonella*. Method I (Scheme 1) outlines TSP-NAEB conjugation through the terminal amine of NAEB to the thiol moiety of the terminal cysteine on TSP.<sup>8</sup> The silica shell of the as-fabricated NAEB is terminated with a hydroxyl functional group which was first converted into amine with diethylenetriamine (DETA). A heterobifunctional cross linker, 6-maleimidohexanoic acid *N*-hydroxysuccinimide ester (NHS-maleimide), is then used to crosslink the amine terminated NAEB to the thiol moiety of the terminal cysteine of TSP. As the cost of the NHS-maleimide represents a significant factor in the production of TSP-NAEB, we were prompted to explore alternative reliable crosslinking strategies.

Each TSP contains a genetically engineered polyhistidine tag that can be used for crosslinking with NAEB as outlined in Methods II and III of Scheme 1. Polyhistidine sequences are commonly introduced into proteins to facilitate purification with immobilized metal-affinity chromatography.<sup>9</sup> It is well established that polyhistidine tags interact strongly with divalent metals such as Ni<sup>2+</sup>, Zn<sup>2+</sup>, Fe<sup>2+</sup> or Cu<sup>2+</sup>.<sup>10</sup> In order to take advantage of such interactions, we need to modify the surface of NAEB to incorporate these divalent metals. Inspired by the common crosslinking protocol used in conjugating the



**Scheme 1** A schematic depiction of NAEB and TSP cross-linking strategies. Method I utilizes NHS-maleimide to cross-link the NH<sub>2</sub>-terminated NAEB to the terminal cysteine of TSP. Method II implants Zn<sup>2+</sup> ions on the silica shell of NAEB followed by conjugation with the polyhistidine of TSP. Method III modifies the COOH-terminated NAEB with Ni<sup>2+</sup> activated HRP which then binds with the polyhistidine of TSP.

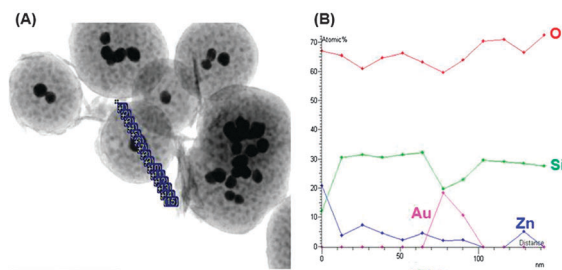


**Fig. 2** STEM (A) and atomic composition (B) as characterized by EDX of the Zn<sup>2+</sup> ion implanted NAEB.

polyhistidine tag onto ZnS coated II–IV quantum dots,<sup>11</sup> the surface of NAEB is modified through sonochemical means to implant Zn<sup>2+</sup> into the silica shell.<sup>12</sup> This was achieved by first sonicating the hydroxyl-terminated NAEB in the presence of zinc acetate [Zn(ac)<sub>2</sub>]. It is proposed that solute radicals are produced under sonochemical conditions as outlined in ref. 12. The solute radicals can easily react with silanol species on the surface of NAEB, thereby yielding the Zn<sup>2+</sup> implanted NAEB. The Zn<sup>2+</sup> implanted NAEB is characterized using TEM and energy dispersive X-ray spectroscopy (EDX) as shown in Fig. 2A and B. The atomic composition of a single NAEB (Fig. 2B) is extrapolated from 12 EDX spectra acquired at the marked position shown in Fig. 2A. In addition to the dominant components of a typical NAEB (O, Si, Au), Fig. 2B also showed a sizeable (5–20%) presence of Zn on NAEB with the highest concentration of Zn detected from the edges of the NAEB. This is strong evidence for the Zn<sup>2+</sup> incorporation in the SiO<sub>2</sub> shell. The Zn<sup>2+</sup>-NAEB is then incubated with TSP to produce the TSP-NAEB conjugate as outlined in Method II of Scheme 1.

Alternatively, a commercially available His-probe (ESI†) which incorporates a Ni<sup>2+</sup> activated derivative of horseradish-peroxidase (Ni<sup>2+</sup>-HRP) is immobilized on the COOH-terminated NAEB as outlined in Method III of Scheme 1. This requires the conversion of NH<sub>2</sub>-NAEB into –COOH termination followed by the activation with EDC/NHS before conjugating to the Ni<sup>2+</sup>-HRP (detailed in ESI†). One advantage in the Ni<sup>2+</sup>-HRP conjugated NAEB is that the conjugation can be verified easily by a chromogenic reagent for HRP such as 3,3',5,5'-tetramethylbenzidine (TMB). Fig. S4 (ESI†) shows both control NAEB and Ni<sup>2+</sup>-HRP conjugated NAEB that were verified with a TMB substrate in the presence of H<sub>2</sub>O<sub>2</sub>. A positive conjugation was confirmed by a distinct colour change (Fig. S4, ESI†) in the Ni<sup>2+</sup>-HRP-NAEB. The Ni<sup>2+</sup>-HRP-NAEB is then incubated with TSP to produce the TSP-NAEB conjugate as shown in Method III of Scheme 1.

To further verify the successful TSP-NAEB conjugations and the preservation of the *Salmonella* binding site, we carried out agglutination assays of the TSP-NAEB conjugates with the target (*Salmonella*) and control (*S. aureus*) microorganisms. Fig. S2 (ESI†) outlines the positive agglutination results for all three types of TSP-NAEB conjugates against *Salmonella*. All three types of TSP-NAEBs (as produced by Methods I, II and III) were able to achieve agglutination when incubated with the target *Salmonella* cells. We also performed scanning electron microscopy (SEM) of the *Salmonella* cells labelled with TSP-NAEB obtained directly from the agglutination wells.

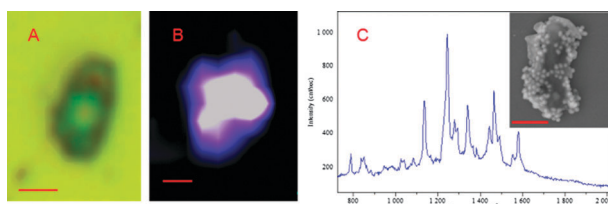


**Fig. 3** SERS detection of single *Salmonella*. A, B and inset of C show the corresponding optical image and SERS intensity map and SEM image of a single NAEB-labelled *Salmonella* cell. SERS spectrum of DTDC NAEB is shown in C. Scale bar is 1  $\mu$ m.

SEM images C, D and E (Fig. S2, ESI $\dagger$ ) show positive binding of TSP-NAEB (prepared by Methods I, II and III, respectively) with *Salmonella* cells. Fig. S2 (ESI $\dagger$ ) also shows control experiments; including the agglutination of control NAEB (without TSP) against *Salmonella* and the TSP-NAEB against control microorganism (*S. aureus*). SEM images F, G (Fig. S2, ESI $\dagger$ ) correspond to the negative binding response of control NAEB (no TSP) against *Salmonella* while image H (Fig. S2, ESI $\dagger$ ) shows the negative binding response of TSP-NAEB against control organism *S. aureus*. Both sets of control experiments showed negative agglutination response. The agglutination studies confirm the following: (1) successful TSP-NAEB conjugation, (2) the specificity of TSP against the target microorganism and (3) reassurance that the three cross-linking strategies described in Scheme 1 preserve the binding sites for the targeted recognition of *Salmonella*.

Fig. 3A shows an optical image of a single *Salmonella* cell labelled with TSP-NAEB produced by Method III: its corresponding SEM image is shown in the inset of Fig. 3C. A corresponding SERS intensity map of the optical image is shown in Fig. 3B. A SERS spectrum of a DTDC Raman reporter molecule taken from a pixel of image B is shown in Fig. 3C. Fig. S3 (ESI $\dagger$ ) shows additional SERS detection of *Salmonella* cells labelled with TSP-NAEB (produced by Methods I and II). In all three conjugation methods, we have demonstrated the successful labelling and subsequent SERS identification of the pathogenic *Salmonella* cells. As demonstrated in Fig. 3 and Fig. S3 (ESI $\dagger$ ), the detection of a single *Salmonella* cell is easily attainable through SERS imaging.

In conclusion, we have demonstrated SERS active TSP-NAEB conjugates that function as highly sensitive and highly specific nanoprobe for the detection of *Salmonella* cells down to a single cell limit. More specifically, we have shown that the silica encapsulation of NAEB serves as a versatile platform for further modification and cross-linking with various moieties of the *Salmonella*-specific TSP. While successful recognition and labelling of *Salmonella* cells were achieved in all of the three types of TSP-NAEB conjugates, Method II highlights, for the first time, the binding of a protein onto a  $Zn^{2+}$  modified silica

nanoparticle without the use of extra crosslinking agents. These SERS-based nanoprobe can be integrated easily into other analytical platforms such as microarray assay or microfluidic based flow cytometry to achieve high throughput screening of pathogenic bacteria.

## Notes and references

- (a) M. K. Fan, G. F. S. Andrade and A. G. Brolo, *Anal. Chim. Acta*, 2011, **693**, 7–25; (b) L. M. Liz-Marzan, M. Giersig and P. Mulvaney, *Langmuir*, 1996, **12**, 4329–4335; (c) C. R. Yonzon, D. A. Stuart, X. Y. Zhang, A. D. McFarland, C. L. Haynes and R. P. Van Duyne, *Talanta*, 2005, **67**, 438–448.
- (a) R. M. Jarvis and R. Goodacre, *Anal. Chem.*, 2004, **76**, 40–47; (b) K. Faulds, W. E. Smith and D. Graham, *Analyst*, 2005, **130**, 1125–1131; (c) L. Zeiri, B. V. Bronk, Y. Shabtai, J. Eichler and S. Efrima, *Appl. Spectrosc.*, 2004, **58**, 33–40; (d) W. R. Premasiri, D. T. Moir, M. S. Klempner, N. Krieger, G. Jones and L. D. Ziegler, *J. Phys. Chem. B*, 2005, **109**, 312–320.
- (a) P. J. Huang, L. L. Tay, J. Tanha, S. Ryan and L. K. Chau, *Chem.–Eur. J.*, 2009, **15**, 9330–9334; (b) P. J. Huang, L. K. Chau, T. S. Yang, L. L. Tay and T. T. Lin, *Adv. Funct. Mater.*, 2009, **19**, 242–248.
- (a) N. J. Halas, S. Lal, W. S. Chang, S. Link and P. Nordlander, *Chem. Rev.*, 2011, **111**, 3913–3961; (b) L. L. Tay, J. Hulse, D. Kennedy and J. P. Pezacki, *J. Phys. Chem. C*, 2010, **114**, 7356–7363; (c) K. L. Wustholz, A. I. Henry, J. M. McMahon, R. G. Freeman, N. Valley, M. E. Piotti, M. J. Natan, G. C. Schatz and R. P. Van Duyne, *J. Am. Chem. Soc.*, 2010, **132**, 10903–10910; (d) H. X. Xu, J. Aizpurua, M. Kall and P. Apell, *Phys. Rev. E*, 2000, **62**, 4318–4324.
- 5 S. Ryan, A. J. Kell, H. van Faassen, L. L. Tay, B. Simard, R. MacKenzie, M. Gilbert and J. Tanha, *Bioconjugate Chem.*, 2009, **20**, 1966–1974.
- 6 (a) S. Waseh, P. Hanifi-Moghaddam, R. Coleman, M. Masotti, S. Ryan, M. Foss, R. MacKenzie, M. Henry, C. M. Szymanski and J. Tanha, *PLoS One*, 2010, **5**(11), e13904; (b) A. Singh, S. K. Arya, N. Glass, P. Hanifi-Moghaddam, R. Naidoo, C. M. Szymanski, J. Tanha and S. Evoy, *Biosens. Bioelectron.*, 2010, **26**, 131–138.
- 7 (a) S. Steinbacher, R. Seckler, S. Miller, B. Steipe, R. Huber and P. Reinemer, *Science*, 1994, **265**, 383–386; (b) J. King, C. Haase-Pettingell, A. S. Robinson, M. Speed and A. Mitraki, *FASEB J.*, 1996, **10**, 57–66; (c) S. Steinbacher, U. Baxa, S. Miller, A. Weintraub, R. Seckler and R. Huber, *Proc. Natl. Acad. Sci. U. S. A.*, 1996, **93**, 10584–10588; (d) B. L. Chen and J. King, *Biochemistry*, 1991, **30**, 6260–6269.
- 8 (a) M. Zhou, E. Nakatani, L. S. Gronenberg, T. Tokimoto, M. J. Wirth, V. J. Hruby, A. Roberts, R. M. Lynch and I. Ghosh, *Bioconjugate Chem.*, 2007, **18**, 323–332; (b) G. Mattson, E. Conklin, S. Desai, G. Nielander, M. D. Savage and S. Morgensen, *Mol. Biol. Rep.*, 1993, **17**, 167–183.
- 9 (a) E. K. M. Ueda, P. W. Gout and L. Morganti, *J. Chromatogr. A*, 2003, **988**, 1–23; (b) X. S. Sun, J. F. Chiu and Q. Y. He, *Expert Rev. Proteomics*, 2005, **2**, 649–657.
- 10 V. Gaber-Porekar and V. Menart, *J. Biochem. Biophys. Methods*, 2001, **49**, 335–360.
- 11 (a) K. E. Sapsford, I. L. Medintz, J. P. Golden, J. R. Deschamps, H. T. Uyeda and H. Mattoussi, *Langmuir*, 2004, **20**, 7720–7728; (b) K. E. Sapsford, T. Pons, I. L. Medintz, S. Higashiyama, F. M. Brunel, P. E. Dawson and H. Mattoussi, *J. Phys. Chem. C*, 2007, **111**, 11528–11538.
- 12 (a) M. L. Breen, A. D. Dinsmore, R. H. Pink, S. B. Qadri and B. R. Ratna, *Langmuir*, 2001, **17**, 903–907; (b) N. A. Dhas, A. Zaban and A. Gedanken, *Chem. Mater.*, 1999, **11**, 806–813.